


Splitting the local Hilbert space: Matrix product state based approach to large local dimensions

Naushad Ahmad Kamar  and Mohammad Maghrebi

Department of Physics and Astronomy, Michigan State University, East Lansing, Michigan 48824, USA

 (Received 30 November 2023; revised 23 July 2024; accepted 24 July 2024; published 8 August 2024)

A large, or even infinite, local Hilbert space dimension poses a significant computational challenge for simulating quantum systems. In this work, we present a matrix product state (MPS) based method for simulating one-dimensional quantum systems with a large local Hilbert space dimension, an example being bosonic systems with a large on-site population. To this end, we *split* the local Hilbert space corresponding to one site into two sites, each with a smaller Hilbert space dimension. An advantage of this method is that it can be easily integrated into MPS based techniques such as time-dependent variational principle (TDVP) without changing their standard algorithmic structure. Here, we implement our method using the TDVP to simulate the dynamics of the spin-boson model, a prototypical model of a spin interacting with a large bath of bosonic modes. We benchmark our method against and find excellent agreement with previous studies.

DOI: [10.1103/PhysRevB.110.075114](https://doi.org/10.1103/PhysRevB.110.075114)

I. INTRODUCTION

Characterizing the interaction between the bosonic modes and electronic or spin degrees of freedom is essential for understanding properties of materials [1,2], including superconductivity [3]. A well-known example is the effect of electron-phonon coupling on the mass of electrons, which leads to the emergence of quasiparticles known as polarons [4]. On the experimental front, circuit QED [5–8] and trapped ions [9,10], among others, provide highly controlled platforms for simulating a broad range of models of interest which also involve bosonic degrees of freedom with tunable coupling. A fundamental goal is to design perfect qubits in these platforms; however, in practice, such qubits are unavoidably coupled with the surrounding environment, which is often considered to be bosonic.

The infinite local Hilbert space dimension of the bath, due to its bosonic nature, presents a significant numerical challenge; an exact diagonalization, even for small systems, would be difficult unless the bosonic population is low, in contrast with spin-1/2 or fermionic chains. To cure this problem, Zhang *et al.* [11] used the largest relevant eigenvalues and the corresponding eigenvectors of the local density matrix to identify an effective local Hilbert space dimension that is smaller than the original one. In general, the local density matrix has d_b eigenvalues with d_b the original local Hilbert space dimension. However, in the ground state, these eigenvalues decrease rapidly; this allows for an approximation of the local density matrix through an optimal local Hilbert space with dimension $d_o \ll d_b$. This method is called local-basis optimization and the corresponding space is the optimal bosonic basis. Various techniques [12–14] that combine local basis optimization and matrix product state (MPS) [15] based methods such as time-evolving block decimation (TEBD) [16], variational matrix product states (VMPS) [15], and time-dependent variational principle (TDVP) [17,18] have been utilized to investigate the ground state and dynamics of quantum systems that involve bosonic degrees of freedom.

However, the local basis optimization changes the standard form of VMPS [13], TEBD [12], and TDVP [14], and modifies their algorithmic structure. For example, in VMPS, TEBD, and TDVP methods, one optimizes the MPS and the matrix corresponding to the orthogonality center of the MPS. However, introducing an optimal bosonic basis, one should also optimize the local Hilbert space [12–14] which drastically changes the structure of these MPS based methods.

In this paper, we propose a simple method to treat a large local Hilbert space dimension without truncating the local density matrix, which preserves the algorithmic structure of VMPS and TDVP techniques. We exploit the sparsity of the Hamiltonian's local matrix product operator (MPO) [15] and split the original local Hilbert space into two smaller ones using a matrix decomposition method, specifically the singular value decomposition. Upon splitting, the system doubles in linear size, but the local Hilbert space dimension reduces to $\sqrt{d_b}$. We apply our proposed method to the spin-boson model [19], which describes the dynamics of a spin-1/2 strongly coupled to an infinite number of bosonic degrees of freedom—this prototypical model emerges in a variety of quantum systems [5–10]. Specifically, we simulate the dynamics by incorporating our method into the TDVP.

The structure of the paper is as follows. In Sec. II, we introduce the spin-boson model and present a mapping to a short-range semi-infinite chain suitable for numerical simulation. In Sec. III, we briefly explain the standard MPS approach and then introduce our main method. We provide numerical results benchmarking our method in Sec. IV and finally conclude and discuss future directions in Sec. V. We provide further details of the MPO decomposition in the Appendix.

II. MODEL

We consider a two-level system S , coupled with an infinite number of noninteracting bosons, famously known as the spin-boson model [19]. We describe the system-bath coupling

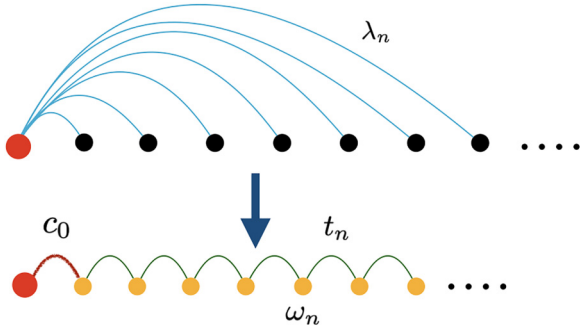


FIG. 1. Two lattice representations of the spin-boson model. The top panel shows the spin-boson model introduced in Eq. (2). The large (red) circle represents the spin and the small (black) circles indicate the bosonic modes. The spin-boson coupling λ_n is denoted by the (blue) curves. In the lower panel, the spin-boson model is shown in the transformed basis given by Eq. (5). The small (orange) circles represent the bosonic modes in the transformed basis that defines a tight binding model with site-dependent energy ω_n and tunneling amplitude t_n . The spin interacts directly with the first bosonic site with a strength c_0 .

via the Hamiltonian

$$H = H_S + H_B + H_{SB}, \quad (1)$$

where the Hamiltonians H_S , H_B , and H_{SB} describe the system, bath, and the linear coupling between the system and the bath, respectively,

$$\begin{aligned} H_S &= -\frac{\Delta}{2}\sigma^x, \\ H_B &= \sum_k \omega_k a_k^\dagger a_k, \\ H_{SB} &= \frac{\sigma^z}{2} \sum_k \lambda_k (a_k^\dagger + a_k). \end{aligned} \quad (2)$$

The effective coupling between the spin and the bath depends on ω_k and λ_k and is fully characterized by the spectral function $J(\omega)$ defined as

$$J(\omega) = \pi \sum_k \lambda_k^2 \delta(\omega - \omega_k). \quad (3)$$

Depending on its form, the spectral function could describe a wide range of different qualitative behavior. A representative class of quantum baths are described by the spectral function

$$J(\omega) = 2\pi\alpha\omega^s \omega_c^{1-s} \Theta(\omega_c - \omega), \quad (4)$$

corresponding to an Ohmic bath with $s = 1$ and sub-(super-)Ohmic baths where $s < 1$ ($s > 1$). The parameters α and ω_c characterize the coupling strength and the frequency cut-off of the bath, respectively. For an Ohmic bath, $s = 1$, this model exhibits a quantum phase transition from a delocalized to localized state at $\alpha \simeq 1 + O(\Delta/\omega_c)$ [13,14,19]. Similar quantum phase transitions occur for the sub-Ohmic bath [20,21].

The spin-boson model in Eq. (1) couples the spin to all the bosonic modes, mimicking a kind of long-range interaction, as depicted in the upper panel of Fig. 1; this makes a

simulation based on matrix product states rather expensive. However, by using an appropriate basis transformation of the bosonic local operators $a(a^\dagger)$, this model can be mapped to a nearest-neighbor Hamiltonian as [20,22]

$$\begin{aligned} H &= -\frac{\Delta}{2}\sigma^x + c_0\sigma^z(b_0 + b_0^\dagger) + \sum_{n=0}^L \omega_n b_n^\dagger b_n \\ &+ \sum_{n=0}^{L-1} t_n (b_n^\dagger b_{n+1} + \text{H.c.}), \end{aligned} \quad (5)$$

where b_n 's define the bosonic operators in the new basis and ω_n , t_n , and c_0 denote the local energy, site-dependent tunneling amplitude, and the coupling between the spin and the first site in the bath in the new basis; see also the lower panel of Fig. 1. The above coefficients can be computed exactly and are given by [22]

$$\begin{aligned} \omega_n &= \frac{\omega_c}{2} \left(1 + \frac{s^2}{(s+2n)(2+s+2n)} \right), \\ t_n &= \frac{\omega_c(1+n)(1+s+n)}{(s+2+2n)(3+s+2n)} \sqrt{\frac{3+s+2n}{1+s+2n}}, \\ c_0 &= \sqrt{\frac{\alpha}{2(1+s)}} \omega_c. \end{aligned} \quad (6)$$

While being local, this model comprises bosonic modes whose population can be large, thus posing a challenge for numerical simulation. In the next section, we introduce an MPO decomposition to split a large local Hilbert space into smaller ones. Combined with MPS based methods, this allows us to simulate systems with a large on-site bosonic population.

III. METHOD

In this section, we briefly introduce the MPS and MPO [15] in order to simulate the spin-boson model. The state of the spin-boson model in the MPS language is given by

$$|\psi\rangle = \sum_{\sigma_0, \sigma_1, \dots, \sigma_L} A^{\sigma_0}[0] A^{\sigma_1}[1] \dots A^{\sigma_L}[L] |\sigma_0, \sigma_1, \dots, \sigma_L\rangle, \quad (7)$$

where σ_0 runs from 1 to d and $\sigma_{1,2,\dots,L}$ run from 1 to d_b , where d and d_b are the local Hilbert space dimension of the spin and bosons, respectively. The size of the A matrices ($\chi \times \chi$) bounds the maximum entanglement that can exist in the system. In a similar fashion, an operator can also be defined using a product of operators known as MPO. In general, the MPO of a given Hamiltonian can be constructed as

$$\begin{aligned} H &= \sum_{\sigma_u/l_0, \dots, \sigma_u/l_L} W_{\sigma_{l_0}}^{\sigma_{u0}}[0] W_{\sigma_{l_1}}^{\sigma_{u1}}[1] \dots W_{\sigma_{l_L}}^{\sigma_{uL}}[L] \\ &\times |\sigma_{u0}, \sigma_{u1}, \dots, \sigma_{uL}\rangle \langle \sigma_{l_0}, \sigma_{l_1}, \dots, \sigma_{l_L}|, \end{aligned} \quad (8)$$

where σ_u/l_n denotes the ket/bra indices on site n . For the spin-boson model, the W matrices in the MPO are explicitly given

by

$$\begin{aligned}
 W[0] &= (I_s \quad \sigma^z \quad 0 \quad 0 \quad -\frac{\Delta}{2}\sigma^x), \\
 W[1] &= \begin{pmatrix} I_b & 0 & b^\dagger & b & \omega_0 n_b \\ 0 & 0 & 0 & 0 & c_0(b^\dagger + b) \\ 0 & 0 & 0 & 0 & t_0 b \\ 0 & 0 & 0 & 0 & t_0 b^\dagger \\ 0 & 0 & 0 & 0 & I_b \end{pmatrix}, \\
 W[1 < n < L] &= \begin{pmatrix} I_b & 0 & b^\dagger & b & \omega_{n-1} n_b \\ 0 & 0 & 0 & 0 & 0 \\ 0 & 0 & 0 & 0 & t_{n-1} b \\ 0 & 0 & 0 & 0 & t_{n-1} b^\dagger \\ 0 & 0 & 0 & 0 & I_b \end{pmatrix}, \\
 W[L] &= \begin{pmatrix} \omega_{L-1} n_b \\ 0 \\ t_{L-1} b \\ t_{L-1} b^\dagger \\ I_b \end{pmatrix}.
 \end{aligned} \tag{9}$$

Here, I_s and I_b refer to the identity operators for the spin and the bath, respectively; I_s is a 2×2 matrix for the spin-1/2, while I_b is a $d_b \times d_b$ matrix. We have also defined the local number operator on a given site in the bath as $n_b = b^\dagger b$. The MPO of the spin-boson model, as described in Eq. (9), is a 5×5 matrix of operators defined in the local Hilbert space. In the MPS based methods such as VMPS and one site TDVP, the computational complexity scales with the size of the local Hilbert space dimension d_b , MPS bond dimension χ , and MPO bond dimension X_W as $O(d_b \chi^3 + d_b^2 X_W^2 \chi^3)$ [14,15].

Therefore, for a large d_b , these methods become computationally expensive. To circumvent this problem, we break up, or split, the local Hilbert space \mathcal{H} into two Hilbert spaces, $\mathcal{H} = \mathcal{H}' \otimes \mathcal{H}''$, each with a smaller dimension. A basis state $|\sigma\rangle$ in \mathcal{H} can be then expressed as a product state

$$|\sigma\rangle = |\sigma'\rangle \otimes |\sigma''\rangle, \tag{10}$$

where $|\sigma'\rangle$ and $|\sigma''\rangle$ are defined in \mathcal{H}' and \mathcal{H}'' , respectively, and the corresponding indices σ' , σ'' run from 1 to $\sqrt{d_b}$. There are of course many ways to split the original basis; here, we choose a particular factorization scheme where

$$\sigma = \sqrt{d_b}(\sigma' - 1) + \sigma''. \tag{11}$$

Such a splitting scheme can easily be implemented using, for example, the Numpy's reshape library. Next, the state $|\psi\rangle$ in Eq. (7) can be recast in the new basis as

$$\begin{aligned}
 |\psi\rangle &= \sum_{\sigma_0, \sigma'_1, \sigma''_1, \dots, \sigma'_L, \sigma''_L} A^{\sigma_0} [0] \tilde{A}^{\sigma'_1} [1] \tilde{A}^{\sigma''_1} [2] \dots \\
 &\quad \times \tilde{A}^{\sigma'_L} [2L-1] \tilde{A}^{\sigma''_L} [2L] |\sigma_0, \sigma'_1, \sigma''_1, \dots, \sigma'_L, \sigma''_L\rangle,
 \end{aligned} \tag{12}$$

where we have introduced the new matrices \tilde{A} now spanning sites 1 to $2L$. Each site being split into two, the linear size of the chain is doubled.

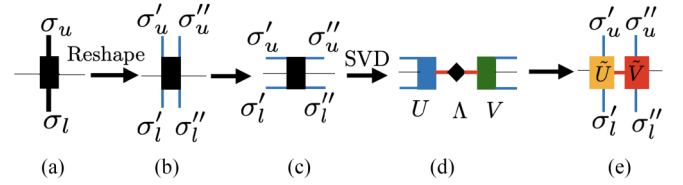


FIG. 2. Schematics of the MPO decomposition. In panel (a), an MPO is shown in the original basis $|\sigma_u\rangle|\sigma_l\rangle$. In panels (b), (c), we reshape the MPO matrix as $W_{\sigma'_l}^{\sigma_u}(w_{i-1}, w_i) \rightarrow W_{\sigma'_l \sigma''_l}^{\sigma'_u \sigma''_u}(w_{i-1}, w_i) \rightarrow W[\sigma'_u \sigma'_l w_{i-1}, \sigma''_u \sigma''_l w_i]$ first in the split basis spanned by $|\sigma'\rangle$ and $|\sigma''\rangle$ and then into a matrix form, where w_i is the index of the MPO bond dimension. In panel (d), we split this matrix using an SVD resulting in the left singular matrix U , singular values Λ , and the right singular matrix V . Finally, in panel (e), we absorb the singular values in the left and right singular matrices as $\tilde{U} = U\sqrt{\Lambda}$ and $\tilde{V} = \sqrt{\Lambda}V$. In this process, we have split a given site's MPO W into two sites with the MPOs \tilde{U} and \tilde{V} .

The local MPO matrices W can also be expressed in the new basis by using singular value decomposition (SVD) as

$$W = U \Lambda V, \tag{13}$$

where the matrix U and V are defined in the new basis spanned by $|\sigma'\rangle$ and $|\sigma''\rangle$, respectively. We leave the technical details to the Appendix; for a schematic explanation, see Fig. 2. For simplicity, we can absorb the diagonal matrix Λ containing the singular values of the SVD into the definition of the U and V matrices as

$$\tilde{U} = U\sqrt{\Lambda}, \quad \tilde{V} = \sqrt{\Lambda}V, \tag{14}$$

upon which Eq. (13) simply becomes

$$W = \tilde{U} \tilde{V}. \tag{15}$$

The column (row) dimension of \tilde{U} (\tilde{V}) is $d_b X_W$, where X_W is the MPO bond dimension before splitting; e.g., $X_W = 5$ for the spin-boson model.

It should be noted that we can further split into multiple sites depending on the problem of interest [23]. We further remark that an alternative would be to directly split the Hamiltonian in the new basis (where each site is split into two sites), but this would lead to a longer-range interaction (e.g., four-body terms) and thus a larger MPO bond dimension and is less optimal compared to the approach presented here.

In practice, however, the effective MPO bond dimension in the split basis could be taken to be much smaller as the singular values Λ_k of the matrix Λ decay rather quickly with the index k . As a representative example, we consider the spin-boson model with $d_b = 100$, $\omega_c = 1$, $\Delta = 0.1$, $s = 1$, and $\alpha = 1.0$, and show Λ_k in descending order in Fig. 3. We observe that Λ_k rapidly decreases and is practically vanishing beyond $k = 29$, therefore effectively 29 instead of $X_W d_b = 500$; the row (column) dimension of \tilde{U} (\tilde{V}) is still $X_W = 5$ since the MPO structure has not changed on the original bonds before splitting. MPS and MPO play a crucial role in MPS based techniques such as VMPS, TDVP, TEBD, and MPO-MPS time evolution [24,25]. In our approach, we have split the original local Hilbert space into local Hilbert spaces with smaller dimensions while leaving the algorithmic

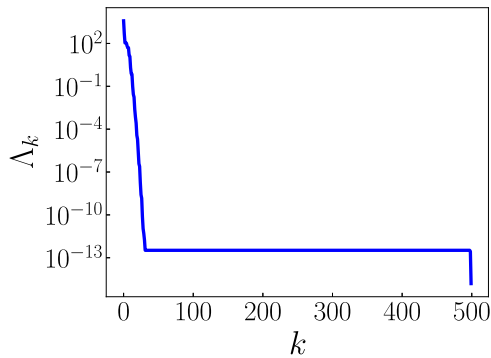


FIG. 3. Singular values of an MPO of the spin-boson model at site $n = 2$ on a semilog scale for $d_b = 100$, $\alpha = 1.0$, $\omega_c = 1.0$, $\Delta = 0.1$, and $\omega_c = 1$. The MPO is shown on site $n = 2$; we find similar behavior on all sites. The singular values decrease exponentially with k and are effectively zero beyond $k = 29$. The MPO bond dimension in the split basis is an order of magnitude smaller than its maximum value of $X_W d_b = 500$.

structure of the MPS intact in the new basis. The only difference is that the MPS is now optimized with the smaller local Hilbert space dimension of $\sqrt{d_b}$ in the split basis. In the single site TDVP, the main computational complexity comes from singular value decomposition (SVD) of MPS to bring it to a canonical form as well as the construction of the local effective Hamiltonian. While the computational complexity due to the SVD of MPS and that of the effective Hamiltonian scale as $O(d_b \chi^3)$ [14] and $O(d_b^2 \chi^3 X_W^2)$ [15] in the original basis, respectively, they scale as $O(2d_b^{1/2} \chi^3)$ and $O(2d_b \chi^3 X_W'^2)$ in the new basis, where the factor of 2 is due to the system size being doubled and X_W' is the MPO bond dimension after splitting. We should note that the computational cost due to MPO bond dimension would be even faster because of the sparse nature of the MPO. We thus expect that the split basis features a speedup by a factor of the order of $O(d_b)$ compared to the old basis for a large d_b at a fixed χ ; this is a massive speedup for large local Hilbert space dimensions. Overall the computational complexity in the new basis scales as $O(d_b^{1/2} \chi^3 + d_b X_W'^2 \chi^3)$ [14,15].

In Fig. 4, we show the CPU time per sweep of the TDVP as a function of d_b both with and without the splitting of the local Hilbert space. Indeed, we find that the scaling with d_b is qualitatively consistent with the theoretical scaling presented above with increasing d_b (the bond dimension is $\chi = 10$).

We should note that the MPO bond dimension also increases upon splitting which could effect the computational cost to construct the effective Hamiltonian. The computational cost due to the MPO bond dimension scales as $O(d_b^2 X_W^2 \chi^3)$ in the original basis [15] and $O(d_b X_W'^2 \chi^3)$ in the split basis. The corresponding ratio is $d_b (X_W / X_W')^2 \approx 3$ for $d_b = 100$, so we still get a speedup for MPO tensor contractions despite the increase in the MPO bond dimension. In practice, the computational advantage should be higher because of the sparse nature of the MPO. We note that a similar approach has been used for the Hubbard-Holstein model with VMPS, as stated in Ref. [23]. However, while Ref. [23] mainly focuses on the physics of the Hubbard-Holstein model and briefly mentions the splitting of local Hilbert space basis, our analysis

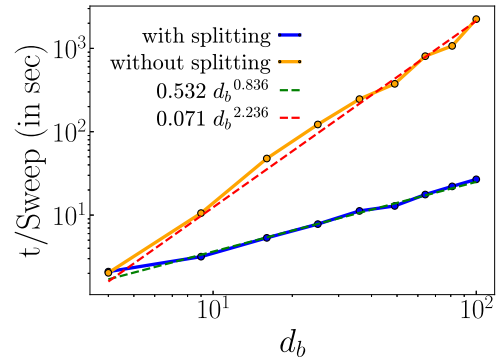


FIG. 4. CPU time per TDVP sweep as a function of d_b (the local Hilbert space dimension) on the log-log scale with and without the splitting of the local Hilbert space; here, $s = 0.5$ and $\chi = 10$. The CPU time shows power-law dependence on d_b ; see the dashed line and the fit in the legends. We find that, with the splitting, the computational cost is reduced by more than an order of magnitude for large d_b compared to the original TDVP method.

provides a detailed approach to splitting the local Hilbert space. Moreover, we concentrate on time-evolution using TDVP for the spin-boson model, whereas Ref. [23] concentrates on VMPS.

In the next section, we use the spin-boson model as a testbed for our method.

IV. RESULTS

In this section, we apply our method to the spin-boson model and specifically study the dynamics of the spin. We start from an initial state at $t = 0$ where the spin is in the $|\uparrow\rangle$ state (in the σ^z basis) and the bosonic modes are in their vacuum state,

$$|\psi(0)\rangle = |\uparrow\rangle \otimes |0\rangle \otimes \cdots \otimes |0\rangle, \quad (16)$$

where $b|0\rangle = 0$ and $\sigma^z|\uparrow\rangle = |\uparrow\rangle$. We are mainly interested in the time evolution of magnetization defined by $\langle \sigma^z(t) \rangle = \langle \psi(t) | \sigma^z | \psi(t) \rangle$, where

$$|\psi(t)\rangle = e^{-iHt} |\psi(0)\rangle. \quad (17)$$

In order to compute $|\psi(t)\rangle$, we employ the TDVP algorithm in the new basis. We fix the interaction parameters at $\Delta = 0.1$, $d_b = 100$, $\omega_c = 1$, $L = 100$, and take the MPS bond dimension $\chi = 5$. We study the dynamics for both Ohmic ($s = 1$) and sub-Ohmic (with $s = 0.5$) baths. In Fig. 5, we depict $\langle \sigma^z(t) \rangle$ as a function of time for different values of the interaction parameters in the range $\alpha = 0.1-1.5$ and for $s = 1$. For $\alpha = 0.1-0.4$, we find that the dynamics is underdamped; see the upper panel of Fig. 5. The frequency of oscillations decreases while the damping rate increases with α , in harmony with the previous studies [19,26–28]. Specifically, the oscillation frequency is renormalized by the spin-bath coupling α as $\Delta_r = \Delta(\Delta/\omega_c)^{\frac{\alpha}{1-\alpha}}$ [19,26–28]; we have verified that our results are in quantitative agreement with this equation. For $\alpha = 0.5, 0.7$, we observe that $\langle \sigma^z(t) \rangle$ decays exponentially to zero, a behavior which persists in the range $0.5 \leq \alpha < 1$ [14,19]. At or above the critical point $\alpha_c = 1.0$, the magnetization $\langle \sigma^z(t) \rangle$ barely decays and is localized in the $|\uparrow\rangle$

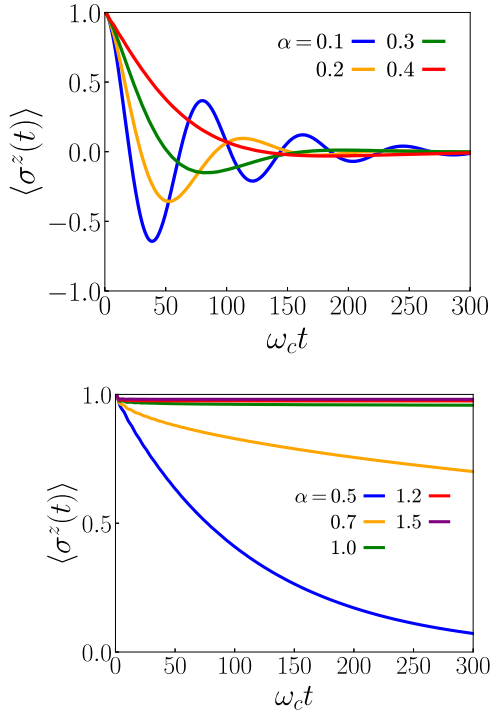


FIG. 5. Magnetization $\langle \sigma^z(t) \rangle$ as a function of time in the presence of an Ohmic bath, $s = 1$, and at different values of α ; we have taken $\Delta = 0.1$ and $\omega_c = 1.0$. The upper panel depicts $\langle \sigma^z(t) \rangle$ for $\alpha = 0.1$ – 0.4 . The spin shows coherent damping as a function of time, with the frequency of oscillations decreasing with α . The lower panel depicts $\langle \sigma^z(t) \rangle$ for $\alpha = 0.5, 0.7, 1.0, 1.2$, and 1.5 . The spin shows incoherent damping as a function of time for $0.5 \leq \alpha < 1$. At and beyond the critical point $\alpha_c = 1.0$, the dynamics is frozen close to $|\uparrow\rangle$, signaling a quantum phase transition from a delocalized to a localized phase.

state; see the lower panel of Fig. 5. This signals a quantum phase transition from a delocalized to a localized state, again consistent with the previous results [14,19,20].

As another example, we consider the dynamics of the spin coupled to a sub-Ohmic bath. In Fig. 6, we show $\langle \sigma^z(t) \rangle$ as a function of time in the presence of a sub-Ohmic bath with $s = 0.5$ and for $\alpha = 0.005$ – 0.20 . Again, we can identify the underdamped regime (upper panel) as well as the overdamped and localized regimes (lower panel). We find that $\langle \sigma^z \rangle$ saturates to a nonzero value beyond $\alpha = 0.125$, signaling a quantum phase transition to a localized phase, consistent with Ref. [14]. Finally, in Fig. 7, we compare our numerical results with those presented in Ref. [14] for $s = 0.5$ and different values of α . We find that our numerical results exactly match the data presented in Ref. [14], thus providing a nontrivial check of the accuracy and efficiency of our method. An advantage of our method is its simple structure which can be easily integrated into the standard MPS based methods.

V. CONCLUSION AND PERSPECTIVE

We have proposed a simple computational approach to simulate systems involving a large local Hilbert space dimension. Our method is based on splitting a large local Hilbert space into two sites with a smaller dimension. We have shown

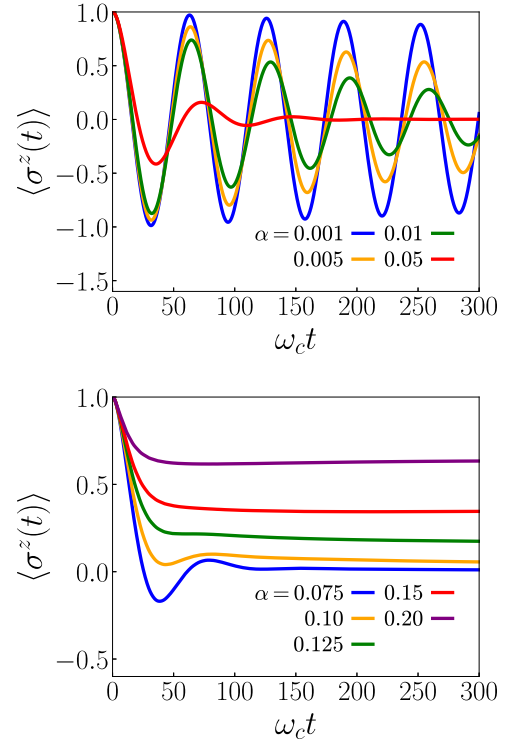


FIG. 6. Magnetization $\langle \sigma^z(t) \rangle$ as a function of time in the presence of a sub-Ohmic bath with $s = 0.5$ and at different values of α ; we have taken $\Delta = 0.1$ and $\omega_c = 1$. The upper panel depicts the $\langle \sigma^z(t) \rangle$ for $\alpha = 0.001$ – 0.05 , which displays coherent damping as a function of time; the oscillation frequency decreases with α similar to the Ohmic case. The lower panel depicts $\langle \sigma^z(t) \rangle$ for $\alpha = 0.075$ – 0.20 . The spin exhibits overdamped dynamics for $\alpha > 0.1$ before it enters the localized phase around $\alpha = 0.125$.

that our approach correctly reproduces the results obtained from the TDVP combined with the local basis optimization for the spin-boson model [14]. Our method has the advantage that it does not change the algorithmic structure of MPS based

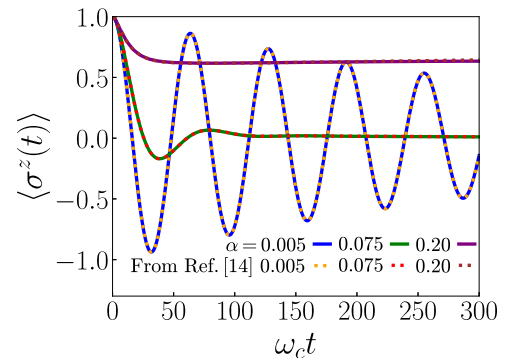


FIG. 7. Magnetization $\langle \sigma^z(t) \rangle$ as a function of time in the presence of the sub-Ohmic bath at different values of α , and with $\Delta = 0.1$, $\omega_c = 1.0$, and $s = 0.5$. Our results (the solid lines) are contrasted against the data taken from Ref. [14] (dotted lines), which are obtained using TDVP combined with the optimal bosonic basis. The excellent agreement with this data is a nontrivial check of our method.

methods, in contrast with MPS approaches that utilize the local basis optimization [12–14].

Our numerical method becomes even more vital in simulating bosonic systems described by a mixed state either at finite temperature or in open quantum systems, e.g., in systems described by the Lindblad master equation. In these scenarios, one generally vectorizes the density matrix in order to bring it to a form that can be represented in the MPS form; however, the local Hilbert space dimension becomes the square of the original local Hilbert space dimension, which could pose a challenge for numerical simulations (see also [29]). Our approach provides a formidable alternative to simulate systems described by a large local Hilbert space dimension.

In this work, we have proposed a method to treat large local Hilbert spaces by splitting them into smaller ones. It is worthwhile extending this idea to a large *bond dimension* where a local MPS is decomposed into two or more matrices with a smaller bond dimension, leading to ladderlike lattices. Such an approach could result in more efficient MPS based calculations where the original bond dimension is large.

ACKNOWLEDGMENTS

We thank A. Chin for useful discussions. This work is supported by the Air Force Office of Scientific Research (AFOSR) under Award No. FA9550-20-1-0073. We also acknowledge support from the National Science Foundation under the NSF CAREER Award (No. DMR2142866), as well as NSF Grants No. DMR1912799 and No. PHY2112893.

APPENDIX: MPO SPLITTING IN σ' AND σ'' BASIS

In this Appendix, we provide further details for the decomposition of a local MPO in terms of the two MPOs with smaller local Hilbert space dimensions. We first split $|\sigma\rangle$ into $|\sigma'\rangle$ and $|\sigma''\rangle$ as

$$|\sigma\rangle = |\sigma'\rangle \otimes |\sigma''\rangle, \quad (\text{A1})$$

where σ' and σ'' runs from 1 to $\sqrt{d_b}$. We can express the local MPO matrix W as a four-dimensional array of size $d_b \times d_b \times X_W \times X_W$, where X_W is the MPO bond dimension. We express the corresponding array elements as

$$W[\sigma_u, \sigma_l, w_{i-1}, w_i] = W_{\sigma_l}^{\sigma_u}(w_{i-1}, w_i), \quad (\text{A2})$$

where w_i runs from 1 to X_W , and in an abuse of notation we used the same symbol W to denote the array. Splitting the local basis as in Eq. (A1), the above array can be recast as a six-

dimensional array in the new basis:

$$W[\sigma'_u, \sigma''_u, \sigma'_l, \sigma''_l, w_{i-1}, w_i] = W_{\sigma'_l, \sigma''_l}^{\sigma'_u, \sigma''_u}(w_{i-1}, w_i). \quad (\text{A3})$$

We can reshape W again to bring it into the form

$$W[\sigma'_u, \sigma''_u, \sigma'_l, \sigma''_l, w_{i-1}, w_i] \rightarrow W[w_{i-1}, \sigma'_u, \sigma'_l, \sigma''_u, \sigma''_l, w_i]. \quad (\text{A4})$$

Finally we can express W in matrix form as

$$W[w_{i-1}, \sigma'_u, \sigma'_l, \sigma''_u, \sigma''_l, w_i] \rightarrow W[w_{i-1} \sigma'_u \sigma'_l, \sigma''_u \sigma''_l w_i]. \quad (\text{A5})$$

The MPO W can be then factorized using the SVD as

$$\begin{aligned} W[w_{i-1} \sigma'_u \sigma'_l, \sigma''_u \sigma''_l w_i] \\ = \sum_{k=1}^{X_W d_b} U[w_{i-1} \sigma'_u \sigma'_l, k] \Lambda_k V[k, \sigma''_u \sigma''_l w_i]. \end{aligned} \quad (\text{A6})$$

In the above equation k runs from 1 to $X_W d_b$; however, in practice, Λ_k decays rapidly with k and most of the singular values are zeros and we can set the upper limit to some $k_{\text{eff}} < X_W d_b$.

Finally, the above equation can be written as

$$\begin{aligned} W[w_{i-1} \sigma'_u \sigma'_l, \sigma''_u \sigma''_l w_i] &= \sum_{k=1}^{k_{\text{eff}}} U[w_{i-1} \sigma'_u \sigma'_l, k] \Lambda_k V[k, \sigma''_u \sigma''_l w_i] \\ &= \sum_{k=1}^{k_{\text{eff}}} \tilde{U}[w_{i-1} \sigma'_u \sigma'_l, k] \tilde{V}[k, \sigma''_u \sigma''_l w_i], \end{aligned} \quad (\text{A7})$$

where we have defined

$$\begin{aligned} \tilde{U}[w_{i-1} \sigma'_u \sigma'_l, k] &= U[w_{i-1} \sigma'_u \sigma'_l, k] \sqrt{\Lambda_k}, \\ \tilde{V}[k, \sigma''_u \sigma''_l w_i] &= \sqrt{\Lambda_k} V[k, \sigma''_u \sigma''_l w_i]. \end{aligned} \quad (\text{A8})$$

The matrices $\tilde{U}[w_{i-1} \sigma'_u \sigma'_l, k]$ and $\tilde{V}[k, \sigma''_u \sigma''_l w_i]$ in the above equation can again be reshaped as

$$\begin{aligned} \tilde{U}[w_{i-1} \sigma'_u \sigma'_l, k] &\rightarrow \tilde{U}[w_{i-1}, \sigma'_u, \sigma'_l, k] \rightarrow \tilde{U}[\sigma'_u, \sigma'_l, w_{i-1}, k], \\ \tilde{V}[k, \sigma''_u \sigma''_l w_i] &\rightarrow \tilde{V}[k, \sigma''_u, \sigma''_l, w_i] \rightarrow \tilde{V}[\sigma''_u, \sigma''_l, k, w_i], \end{aligned} \quad (\text{A9})$$

where \tilde{U} and \tilde{V} represent the MPO in $|\sigma'\rangle$ and $|\sigma''\rangle$ basis, respectively. In the new basis the MPO of the split sites can be then expressed as

$$W = \tilde{U} \tilde{V}. \quad (\text{A10})$$

A schematic figure summarizing the above steps is illustrated in Fig. 2.

[1] D. N. Basov, R. D. Averitt, D. van der Marel, M. Dressel, and K. Haule, *Rev. Mod. Phys.* **83**, 471 (2011).
[2] K. Yonemitsu and K. Nasu, *Phys. Rep.* **465**, 1 (2008).

[3] F. Marsiglio and J. P. Carbotte, in *Superconductivity*, edited by K. H. Bennemann and J. B. Ketterson (Springer, Berlin, Heidelberg, 2008), pp. 73–162.

- [4] R. P. Feynman, *Phys. Rev.* **97**, 660 (1955).
- [5] P. Forn-Díaz, J. J. García-Ripoll, B. Peropadre, J.-L. Orgiazzi, M. Yurtalan, R. Belyansky, C. M. Wilson, and A. Lupascu, *Nat. Phys.* **13**, 39 (2017).
- [6] L. Magazzù, P. Forn-Díaz, R. Belyansky, J.-L. Orgiazzi, M. Yurtalan, M. R. Otto, A. Lupascu, C. Wilson, and M. Grifoni, *Nat. Commun.* **9**, 1403 (2018).
- [7] F. Yoshihara, T. Fuse, S. Ashhab, K. Kakuyanagi, S. Saito, and K. Semba, *Nat. Phys.* **13**, 44 (2017).
- [8] M. Mirhosseini, E. Kim, X. Zhang, A. Sipahigil, P. B. Dieterle, A. J. Keller, A. Asenjo-Garcia, D. E. Chang, and O. Painter, *Nature (London)* **569**, 692 (2019).
- [9] D. Porras, F. Marquardt, J. von Delft, and J. I. Cirac, *Phys. Rev. A* **78**, 010101(R) (2008).
- [10] A. Lemmer, C. Cormick, D. Tamascelli, T. Schaetz, S. F. Huelga, and M. B. Plenio, *New J. Phys.* **20**, 073002 (2018).
- [11] C. Zhang, E. Jeckelmann, and S. R. White, *Phys. Rev. Lett.* **80**, 2661 (1998).
- [12] C. Brockt, F. Dorfner, L. Vidmar, F. Heidrich-Meisner, and E. Jeckelmann, *Phys. Rev. B* **92**, 241106(R) (2015).
- [13] C. Guo, A. Weichselbaum, J. von Delft, and M. Vojta, *Phys. Rev. Lett.* **108**, 160401 (2012).
- [14] F. A. Y. N. Schröder and A. W. Chin, *Phys. Rev. B* **93**, 075105 (2016).
- [15] U. Schollwöck, *Ann. Phys. (NY)* **326**, 96 (2011).
- [16] G. Vidal, *Phys. Rev. Lett.* **93**, 040502 (2004).
- [17] J. Haegeman, J. I. Cirac, T. J. Osborne, I. Pižorn, H. Verschelde, and F. Verstraete, *Phys. Rev. Lett.* **107**, 070601 (2011).
- [18] J. Haegeman, C. Lubich, I. Oseledets, B. Vandereycken, and F. Verstraete, *Phys. Rev. B* **94**, 165116 (2016).
- [19] A. J. Leggett, S. Chakravarty, A. T. Dorsey, M. P. A. Fisher, A. Garg, and W. Zwerger, *Rev. Mod. Phys.* **59**, 1 (1987).
- [20] R. Bulla, N.-H. Tong, and M. Vojta, *Phys. Rev. Lett.* **91**, 170601 (2003).
- [21] M. Vojta, N.-H. Tong, and R. Bulla, *Phys. Rev. Lett.* **94**, 070604 (2005).
- [22] A. W. Chin, Á. Rivas, S. F. Huelga, and M. B. Plenio, *J. Math. Phys.* **51**, 092109 (2010).
- [23] P.-Y. Zhao, K. Ding, and S. Yang, *Phys. Rev. Res.* **5**, 023026 (2023).
- [24] E. Stoudenmire and S. R. White, *New J. Phys.* **12**, 055026 (2010).
- [25] M. P. Zaletel, R. S. K. Mong, C. Karrasch, J. E. Moore, and F. Pollmann, *Phys. Rev. B* **91**, 165112 (2015).
- [26] P. P. Orth, A. Imambekov, and K. Le Hur, *Phys. Rev. B* **87**, 014305 (2013).
- [27] H. Shapourian, *Phys. Rev. A* **93**, 032119 (2016).
- [28] N. A. Kamar, D. A. Paz, and M. F. Maghrebi, *Phys. Rev. B* (to be published), [arXiv:2305.00110](https://arxiv.org/abs/2305.00110).
- [29] S. Wolff, A. Sheikhan, and C. Kollath, *SciPost Phys. Core* **3**, 010 (2020).